NET CIRCULAR POLARIZATION OF SUNSPOT PENUMBRAE - SYMMETRY BREAKING BY ANOMALOUS DISPERSION

D. A. N. Müller, R. Schlichenmaier, O. Steiner, and M. Stix

Kiepenheuer-Institut für Sonnenphysik, 79104 Freiburg, Germany

ABSTRACT

We examine the polarization of spectral lines in the penumbra of sunspots by solving the radiative transfer equation of polarized light for a three-dimensional axially symmetric model atmosphere of a sunspot. The Evershed flow is confined to horizontal magnetic flux tubes obtained from MHD calculations. These are embedded in an inclined background magnetic field. In this work, we concentrate on the Stokes-V profiles and examine the net circular polarization (NCP), $\mathcal{N} = \int V(\lambda)\mathrm{d}\lambda$, of two photospheric spectral lines of neutral iron, Fe I 630.25 nm and Fe I 1564.8 nm. Analyzing spectra at a fixed distance from the spot center, we find that the azimuthal variation of $\mathcal{N}$, $\mathcal{N}(\psi)$, is an *antisymmetric* function of ψ w.r.t. to the line connecting disk center and spot center for Fe I 1564.8 nm, while the variation is predominantly *symmetric* for Fe I 630.25 nm. We show that the antisymmetric variation is caused by anomalous dispersion (rotation of the polarization vector in a magnetized plasma). The different inclination angles lead to a discontinuity in the azimuth of the magnetic field along the line-of-sight. We show that this discontinuity together with the effect of anomalous dispersion produces an antisymmetric component in $\mathcal{N}(\psi)$ which outweighs the symmetric component from the discontinuity for Fe I 1564.8 nm, while it is negligible for Fe I 630.25 nm. We finally compute synthetic NCP maps of a sunspot which offer an explanation for recent observational results.

Key words: sunspots - Sun: magnetic field - Sun: photosphere - Techniques: polarimetric - Techniques: spectroscopic.

1. INTRODUCTION

In order to disentangle the fine structure in sunspot penumbrae, we examine asymmetries in the spectral profiles of Stokes parameters. In general, a velocity gradient or discontinuity along the line-of-sight (LOS) is necessary and sufficient to generate Stokes asymmetries, while a gradient or discontinuity in the magnetic field can significantly alter and enhance the asymmetries (see, e.g., Auer & Heasley, 1978; Sánchez Almeida & Lites, 1992). Here, we restrict ourselves to asymmetry properties of Stokes-V profiles. One way to quantify the asymmetry is the net circular polarization, $\mathcal{N} \equiv \int V(\lambda)\,\mathrm{d}\lambda$, where the integration ranges over a full absorption line. In this contribution, we show results which have been reported recently by Müller (2001) and Schlichenmaier et al. (2002), and will be described in greater detail by Müller et al. (2002).

Measurements of the net circular polarization of sunspot penumbrae in single absorption lines have been presented by Westendorp Plaza et al. (2001) in Fe I 630.25 nm and by Schlichenmaier & Collados (2002) in Fe I 1564.8 nm. Surprisingly, sunspot maps of $\mathcal{N}$ in Fe I 630.25 nm are symmetric w.r.t. the line that connects disk with spot center, while $\mathcal{N}$-maps in Fe I 1564.8 nm do not show that symmetry. Quite contrarily, there is a trend that the latter maps are antisymmetric. To understand this puzzling finding, we investigate the azimuthal dependence of $\mathcal{N}$-maps of corresponding synthetic lines that are calculated on the basis of the moving tube model as proposed by Schlichenmaier et al. (1998, herafter SJS98). We show that the effects of anomalous dispersion (see, e.g., Landolfi & Landi Degl'Innocenti, 1996, hereafter LL96, and references therein) play a crucial role for the creation of $\mathcal{N}$.

2. COORDINATE SYSTEMS

A position in the surface plane of a sunspot can be given in polar coordinates (r, ψ), with r being the distance from spot center and with $\psi = 0°$ and $180°$ corresponding to the line which connects disk and spot center. This line is also referred to as the line-of-symmetry, since, e.g., the map of the line-of-sight velocity component of a radial outflow is symmetric w.r.t. this line. As depicted in Fig. 1, we introduce a local cartesian coordinate system (x', y', z') at (r, ψ). For further details, the reader is referred to Schlichenmaier et al. (2002).

3. THE MODEL

For the computation of synthetic Stokes profiles, we rely on the moving tube model of SJS98. For our calcula-

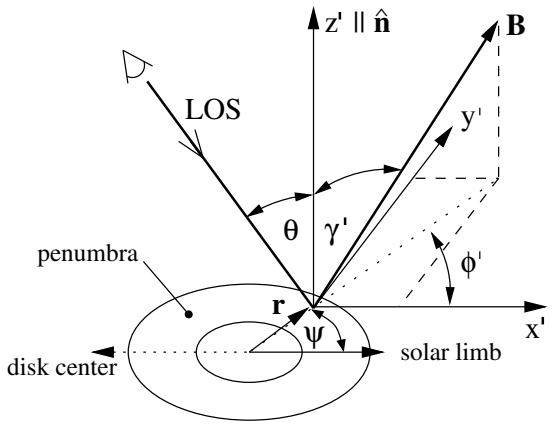

Figure 1. A vector, $\vec{B}$, with polar coordinates (r,ψ) w.r.t. the center of the spot can be described within a local cartesian coordinate system (x',y',z') of which the (x',y')-plane lies in the sunspot surface. The x'-axis is parallel to the line which connects disk and spot center pointing toward the solar limb. The figure sketches the inclination, γ', w.r.t. the surface normal $\hat{n}$ (which is parallel to the z'-axis), and the azimuth, ϕ', w.r.t. the x'-axis of $\vec{B}$. The LOS is within the (x',z')-plane.

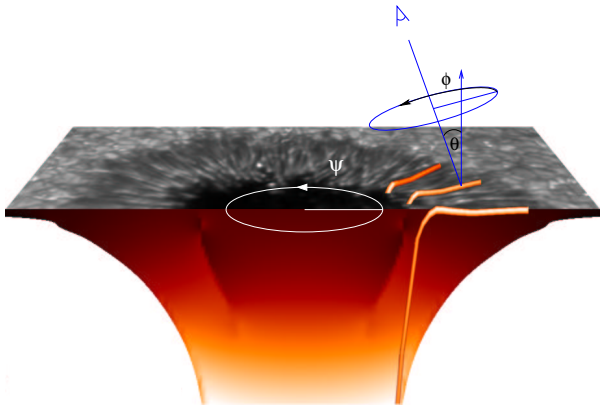

Figure 2. Magnetic flux tubes in the penumbra. For a given heliocentric angle θ, the azimuth ϕ and the inclination γ of the magnetic field vary with the location of the flux tube in the sunspot, characterized by the spot angle ψ.

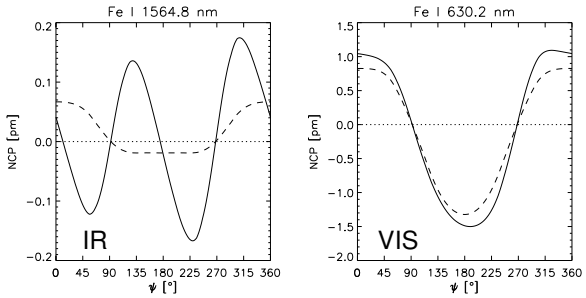

Figure 3. Left panel: $\mathcal{N}(\psi)$ *for Fe I 1564.8 nm and* $r = 12\,000$ km *with* $\theta = 15°$. *Solid line: with anomalous dispersion; dashed line: without anomalous dispersion.* Right panel: *same as left panel, but for Fe I 630.25 nm.*

tions, we use a typical model snapshot with a flux tube breaking through the photosphere in the inner penumbra from where it bends outwards horizontally. An upflow of hot optically thick plasma enters the photosphere along the tube from below. As it flows outwards horizontally, with a flow speed of up to 14 km s^{-1}, it radiatively cools. Since we assume an axially symmetric model sunspot that has no azimuthal component, the azimuth of the magnetic field, ϕ', equals the azimuthal location in the spot, ψ, i.e., $\phi' = \psi$. Along the LOS, the Unno-Rachkovsky-equations for polarized light are integrated numerically for the iron lines at 1564.8 nm and 630.25 nm (details are given in Müller, 2001; Müller et al., 2002). The geometry of tubes for different angles ψ within the sunspot is sketched in Fig. 2.

The presence of a tube embedded in a penumbral background atmosphere causes discontinuities along a line-of-sight transversing it: (1) $\triangle v$, the LOS component of the flow velocity (flow channel embedded in a background at rest), (2) $\triangle\gamma$, the inclination of the magnetic field vector (horizontal flux tube in an inclined background magnetic field), and (3) $\triangle\phi$, the azimuth of the magnetic field vector w.r.t. the LOS. The discontinuity in azimuth, $\triangle\phi$, needs clarification: Although the azimuth of the tube, ϕ'_t, and of the background, ϕ'_b, are the same w.r.t. the local system, $\triangle\phi = \phi_t - \phi_b$ is non-zero (except for $\theta = 0°$ or $\psi = 0°$, 180°) as a consequence of $\gamma'_t \neq \gamma'_b$.

4. NET CIRCULAR POLARIZATION ALONG AN AZIMUTHAL SECTION

With the model described in the preceding section, we calculate synthetic V-profiles along an azimuthal section for a specified radial position (12 000 km). Figure 3 displays the results for Fe I 1564.8 nm (left panel) and for Fe I 630.25 nm (right panel). The calculations are performed with (solid line) and without (dashed line) the effects of anomalous dispersion for $\theta = 15°$. For both lines, $\mathcal{N}(\psi)$ is symmetric w.r.t. the x-axis ($\psi = 0°$ and 180°) if the effects of anomalous dispersion are not taken into account. Including anomalous dispersion, this symmetry is broken. For Fe I 630.25 nm the antisymmetric component is small relative to the symmetric component. However, for Fe I 1564.8 nm the antisymmetric component dominates $\mathcal{N}(\psi)$.

4.1. Symmetry properties of $\mathcal{N}(\psi)$

In order to understand the antisymmetric component in $\mathcal{N}(\psi)$, we consider the symmetry properties of the discontinuities $\triangle v(\psi)$, $\triangle\gamma(\psi)$, and $\triangle\phi(\psi)$ at the interface between the flux tube and the background, which cause the asymmetry in $V(\lambda)$. In our model, $\triangle B$ is negligible at the interface and B decreases only slightly with height. Its influence can therefore be neglected in the following discussion, but we note that $\triangle B(\psi)$ is symmetric and would not alter the following argument.

Properties of $\triangle\phi(\psi)$, $\triangle\gamma(\psi)$, and $\triangle v(\psi)$: Taking into account that $\psi = \phi'$ for an axially symmetric sunspot with no azimuthal components, it is seen from Eqs. (1) – (3) in Schlichenmaier et al. (2002) that $\gamma(\psi)$ and $v(\psi)$ are symmetric, while $\phi(\psi)$ is antisymmetric w.r.t. the transformation $\psi \rightarrow -\psi$. As a consequence, $\triangle\phi(\psi) = \phi_t(\psi) - \phi_b(\psi)$ is antisymmetric, while $\triangle\gamma(\psi)$ and $\triangle v(\psi)$ are symmetric. The appearance of different signs of $\triangle\phi(\psi)$ within a sunspot is sketched in Fig. 4.

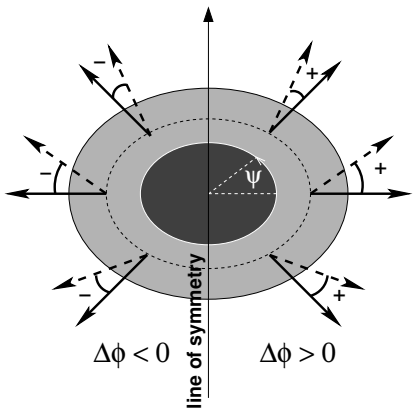

Figure 4. Pictorial representation of the difference in azimuth, $\triangle\phi(\psi)$, between the magnetic field vector inside a flux tube (solid lines) and that of the background field (dashed lines).

$\triangle\phi$ is capable of breaking the symmetry: It has been demonstrated analytically by LL96 that along the LOS a discontinuity in the azimuth of the magnetic field vector is capable of producing a non-vanishing net circular polarization, $\mathcal{N}$. Their formulas reflect that a discontinuity in ϕ along the LOS can produce a non-zero $\mathcal{N}$, if and only if anomalous dispersion is included in the transfer equation of polarized light. Moreover, they demonstrate that the effect of $\triangle\phi$ on $\mathcal{N}$ is proportional to $\sin(2\triangle\phi)$, implying that $\mathcal{N} = \mathcal{N}(\triangle\phi)$ is an antisymmetric function.

Since $\triangle\gamma(\psi)$ and $\triangle v(\psi)$ are both symmetric, $\mathcal{N} = \mathcal{N}(\triangle\gamma(\psi), \triangle v(\psi))$ must also be symmetric w.r.t. ψ. Hence, only $\triangle\phi$ is capable to introduce an antisymmetric component in $\mathcal{N}(\psi)$, i.e., $\mathcal{N}(\psi)$ is composed of a symmetric contribution from $\triangle\gamma(\psi)$ and $\triangle v(\psi)$ (and from $\triangle B(\psi)$, if present) and of an antisymmetric contribution from $\triangle\phi(\psi)$. The latter contributes to $\mathcal{N}$ only if anomalous dispersion is included.

It can be seen in Fig. 3 that the values for $\mathcal{N}$ with and without anomalous dispersion are not identical where $\triangle\phi = 0$, i.e., for $\psi = 0°, 180°$. This means that $\mathcal{N}$, which is solely produced by $\triangle\gamma$ at these locations, depends on whether anomalous dispersion is included or not. In other words, switching on the anomalous dispersion introduces both a symmetric contribution to $\mathcal{N}(\psi)$ and the antisymmetric contribution that is caused by $\triangle\phi$.

4.2. Difference between Fe I 1564.8 nm and Fe I 630.25 nm

Having shown that $\triangle\phi(\psi)$ causes the antisymmetric component in $\mathcal{N}(\psi)$, the question remains, why this effect is small for Fe I 630.25 nm and rather large for Fe I 1564.8 nm. Again, the work of LL96 is of help. They have found an analytical solution for a model with a single discontinuity along the LOS. In their Eqs. (18) and (19), they isolate the effects of $\triangle\gamma$ and $\triangle\phi$ on $\mathcal{N}$ (respectively, $\triangle\theta$, $\triangle\varphi$, v in their article). From these equations it is apparent that the weights of the symmetric contribution from $\triangle\gamma$ and the antisymmetric contribution from $\triangle\phi$ depend on the ratio between the wavelength shift due to the Doppler effect and the magnitude of the Zeeman splitting. Hence, the large difference in wavelength between Fe I 630.25 nm and Fe I 1564.8 nm is responsible for the significant difference between the two lines, since the Doppler effect depends linearly on wavelength, while the Zeeman splitting is proportional to λ^2. Inserting numbers that correspond to our model into the solution of LL96, Müller (2001) estimates that the $\triangle\phi$-effect should dominate $\mathcal{N}$ for Fe I 1564.8 nm and that the $\triangle\gamma$-effect is more important for Fe I 630.25 nm. Hence, although we cannot separate the effects of $\triangle\gamma$ and $\triangle\phi$ on $\mathcal{N}$ in our numerical model, the results presented in Fig. 3 can be understood on the basis of the analytical work of LL96.

4.3. Synthetic NCP maps and comparison with observations

In Fig. 5, we show synthetic maps of the net circular polarization. In the calculations presented here, we have only used the configuration of *one* flux tube, at a time of evolution when it had reached a nearly stationary state. For two heliocentric angles ($\theta = 30°, 45°$), these maps show the NCP at 180 azimuthal positions of the flux tube in the penumbra in steps of $\Delta\psi = 2°$ and for 28 radial positions between $r = 9500$ km and $r = 16\,000$ km. The umbra is not part of the model investigated here, and is set to zero in Fig. 5.

The qualitatively different behavior of the two spectral lines is easily recognized: While the NCP of the spectral line Fe I 630.25 nm is symmetric w.r.t. the line connecting disk center and spot center, the NCP of Fe I 1564.8 nm exhibits a predominantly antisymmetric variation as a function of the spot angle ψ. Moreover, it can be seen that the NCP decreases in the outward direction. This can be explained by the fact that the difference in inclination, $\Delta\gamma$, between the background field and the flux tube declines outwards. The thin concentric rings around $r = 9700$ km are caused by the footpoint of the simulated flux tube which reaches the photosphere at this radial distance. This results in strong gradients in the temperature and the magnetic field, an effect which deserves closer investigation. The amplitude of the NCP of Fe I 630.25 nm is larger than the one of Fe I 1564.8 nm for both heliocentric angles shown in Fig. 5, and the modulus of the NCP of Fe I 630.25 nm is larger on the limb side of the sunspot than on the center side.

Maps of the net circular polarization of sunspot penum-

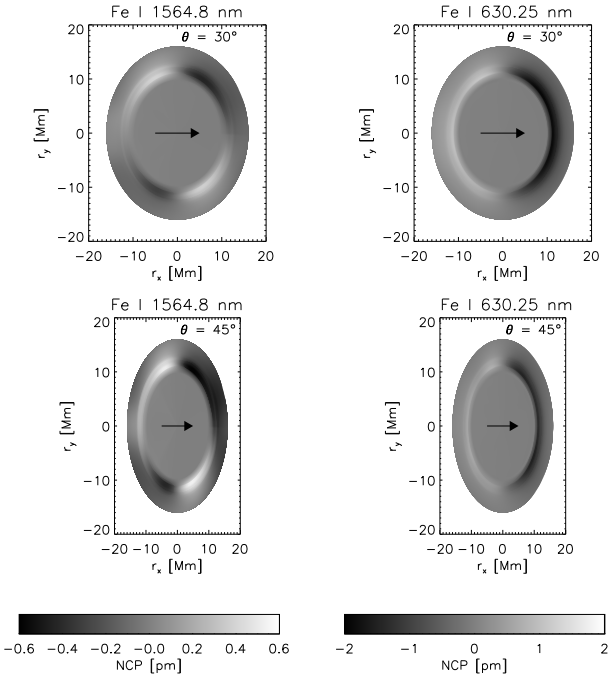

*Figure 5. Synthetic NCP maps of a sunspot for the spectral lines Fe I 1564.8 nm (*left column*) and Fe I 630.25 nm (*right column*) for different heliocentric angles.* Top*:* $\theta = 30°$, bottom*:* $\theta = 45°$. *The black line marks the umbral boundary, the arrows point towards disk center. The footpoint of the flux tube of this model reaches the photosphere at* $r \approx 9700\,km$.

brae have been published by Westendorp Plaza et al. (2001) in Fe I 630.25 nm and by Schlichenmaier & Collados (2002) in Fe I 1564.8 nm. These measurements reveal that in penumbrae, $\mathcal{N}(\psi)$ is essentially symmetric for Fe I 630.25 nm and antisymmetric for Fe I 1564.8 nm. Our theoretical results, based on synthetic lines that emanate from the moving tube model, are in full agreement with these measurements.

5. CONCLUSION

We demonstrate that a discontinuity in the azimuth, $\triangle\phi$, of the magnetic field vector along the line-of-sight together with the effects of anomalous dispersion plays a crucial role for the interpretation of spectropolarimetric measurements in sunspot penumbrae.

In an axially symmetric sunspot in which the magnetic and velocity field vectors have no azimuthal components, a nearly horizontal flow channel embedded in an inclined magnetic background field introduces a discontinuity, $\triangle\phi$, in the azimuth relative to the line-of-sight. Along an azimuthal section within the penumbra, $\triangle\phi(\psi)$ is antisymmetric w.r.t. the line-of-symmetry, giving rise to an antisymmetric contribution to the net circular polarization, $\mathcal{N}(\psi)$. $\mathcal{N}(\psi)$ consists of a symmetric contribution from $\triangle\gamma$ (and $\triangle B$ which, however, is negligible in our model configuration) and an antisymmetric contribution from $\triangle\phi$. The relative weights of these two contributions depend on the ratio of the wavelength shifts induced by the Doppler and Zeeman effect, respectively. The difference between the symmetry properties of $\mathcal{N}$-maps in Fe I 1564.8 nm and Fe I 630.25 nm can therefore be attributed to the large wavelength difference between the two lines.

The striking difference between observed $\mathcal{N}$-maps for the Fe I 1564.8 nm and the Fe I 630.25 nm line can be reproduced by synthetic lines that emanate from a model atmosphere which is based on the moving tube model of SJS98. In this respect, the present work provides strong evidence that magnetic fields with (at least) two different inclinations with different flow velocities are present in the penumbra. It also demonstrates that the spatial distribution of $\mathcal{N}(r,\psi)$ within the penumbra is a valuable diagnostic tool in order to test penumbral models.

REFERENCES

Auer, L. H. & Heasley, J. N. 1978, A&A, 64, 67

Landolfi, M. & Landi Degl'Innocenti, E. 1996, Sol. Phys., 164, 191

Müller, D. A. N., Schlichenmaier, R., Steiner, O., & Stix, M. 2002, A&A, *in preparation*

Müller, D. A. N. 2001, Diploma Thesis, University of Freiburg

Sánchez Almeida, J. & Lites, B. W. 1992, ApJ, 398, 359

Schlichenmaier, R. & Collados, M. 2002, A&A, 381, 668

Schlichenmaier, R., Jahn, K., & Schmidt, H. U. 1998, A&A, 337, 897

Schlichenmaier, R., Müller, D. A. N., Steiner, O., & Stix, M. 2002, A&A, 381, L77

Westendorp Plaza, C., del Toro Iniesta, J. C., Ruiz Cobo, B., Martínez Pillet, V., Lites, B. W., & Skumanich, A. 2001, ApJ, 547, 1130